Progress in Understanding Specimen Size and Geometry Effects on Ductile Fracture

G. P. GIBSON and S. G. DRUCE
Harwell Laboratory, Oxon OX11 0RA, UK

ABSTRACT

In this paper we discuss the effect of specimen size and geometry on ductile crack initiation and growth, using results from previous studies on a C-Mn steel and new results on an aluminium alloy. Experimental evidence is presented to show that the J-R curves for non-sidegrooved specimens comprise contributions from the low crack-tip constraint, near surface, (i.e. shear lip) region, and the high crack-tip constraint, central, (i.e. flat fracture) region of the specimen. Each region has a characteristic J-R curve, which for the shear lip region is apparently independent of specimen size and geometry, and for the flat fracture region is dependent only on the crack tip constraint in the centre of the specimen. The overall J-R curve can be calculated from the two component J-R curves knowing the size of the shear lip as the crack extends. The J-R curve for a given crack tip constraint is apparently independent of whether the plasticity accompanying crack growth is contained within an elastic region or spreads to the specimen boundaries.

KEYWORDS

Fracture: elastic-plastic fracture mechanics; small scale yielding; large scale yielding; crack growth; specimen size; specimen geometry.

INTRODUCTION

One of the objectives of continuing research into fracture mechanics is to improve the transferability of materials toughness properties derived from laboratory tests to structures containing complex crack shapes. A number of studies have been carried out to compare materials toughness properties measured from specimens of differering size and geometry (eg Ernst, 1983, Davis et al, 1983, Ganwood, 1982). Part of the difficulty is that the micromechanisms of ductile fracture and thus the material's toughness depend on the crack tip constraint, which can vary with the size and geometry of the structure (Hancock and Brown, 1980). There are two common situations where the effect of variations in crack-tip constraint have to be

considered. The first concerns relating the toughness properties determined from laboratory test specimens exhibiting large-scale (i.e. non-contained) yielding, to large structures where plasticity is contained within elastically deformed material (i.e. contained yielding). The second concerns the situation of surface intersecting defects, where the crack tip constraint varies around the crack periphery. In this case, crack shape development and the load carrying capacity will depend on the material's resistance to crack growth over a range of crack-tip constraints.

At ICF5, data were presented by one of the authors showing that for a C-Mn steel, the J integral at the onset of crack growth (J_i), and the initial tearing resistance (dJ/da) were influenced by the size and geometry of compact type specimens (Druce, 1981). In particular, a pronounced effect of specimen thickness and sidegrooving on dJ/da was noted. Subsequently, data have been obtained for other specimen geometries including centre-cracked tension (CCT) and double-edge-notched tension (DENT) (Gibson and Druce, 1986 and 1987, Gibson et al, 1987). In addition, crack-tip profile measurements were made to provide a local crack-tip measure of initiation toughness and tearing resistance.

The aim of this paper is to review our current understanding of the effect of specimen size and geometry on crack initiation and growth. The paper is divided into two parts: in the first, a review is given of the size and geometry effects reported previously for a C-Mn steel; in the second, new results on an aluminium alloy are given, comparing J-R curves under contained and non-contained yielding. The results are presented in terms of the Ernst modified J (Ernst, 1983), but the principles discussed apply equally to the crack-growth corrected deformation J.

SPECIMEN SIZE AND GEOMETRY EFFECTS

The results in this section were obtained on a normalised C-Mn steel (BS4360 43A). Experimental details are described briefly below; further details are in (Gibson et al, 1987). J-R curves were obtained from compact specimens of varying widths, (W, 26 to 100mm) and thicknesses, (B, 13 to 50mm), three- and four-point bend specimens (B=25mm, W=50mm), and CCT and DENT specimens (B=W=25mm). The effect of sidegrooving was studied on compact specimens. Specimen testing was carried out to ASTM E813-81. J_i values were calculated from measurements of the critical stretch zone width (SZW_c) in the central region of the specimen, and an empirically determined J versus SZW blunting relationship. The tearing resistance, dJ/da, was obtained from a linear slope to the J-R curve over the initial 2mm of crack growth. A silicone-rubber crack-tip infiltration technique was used to determine the crack opening displacement at the tip of the growing crack (Gibson and Druce, 1987). The size of the shear-lip in the thickness (shear-lip width S), and crack growth (shear-lip length) directions were measured from the fracture surfaces.

A significant effect of specimen size and geometry on the J-R curve was found, with J_i varying by 33% and the J values at 2mm of crack growth varying by 100%. In particular, as shown in Fig. 1, increasing the specimen thickness markedly reduced dJ/da and to a lesser extent J_i. The shear-lip size at a given average crack extension also varied with specimen size and geometry. However, in all cases, the shear-lip width was found to be about 50% greater than the shear lip length, for shear-lip widths smaller than half the specimen thickness. The shear lip width (ie in through thickness

direction) was found to be the same for compact, three- and four-point bend specimens, at a given crack extension and proportional to the square root of the ligament size (b) when b>B, but independent of the specimen thickness. However, the shear-lip size for the tension and bend type geometries were different, being a factor of about 1.4 greater for the CCT and 0.8 smaller for the DENT geometry than for the standard compact geometry of the same thickness.

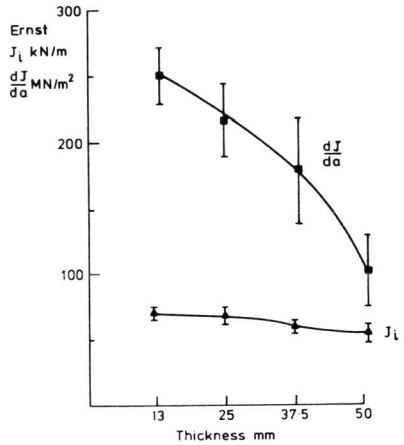

Fig.1. Effect of specimen thickness on toughness.

The presence of flat fracture and shear lip regions on the fracture surface of non-sidegrooved specimens is taken as evidence of a varying crack-tip constraint across the specimen thickness. Adjacent to the specimen sides, there is a region of low crack-tip constraint promoting shear dominated fracture, the width of which is reflected by the width of the shear-lip. In the central region of the specimen, the crack tip constraint is higher, up to that for plane strain in sufficiently thick or suitable sidegrooved specimens. The higher crack-tip constraint promotes a macroscopically flat fracture path. These two regions of differing crack-tip constraint will exhibit different J-R curves and the overall J-R curve will consist of components from the curves for the flat fracture (J_f-R) curve) and shear lip (J_S-R) regions.

$$J = J_f \times \left(1 - \frac{2 \times S}{B}\right) + J_S \times \left(\frac{2 \times S}{B}\right) \qquad (1)$$

The J_f-R curve is dependent on the precise crack-tip constraint in the central region of the specimen and can be determined for one level of constraint from specimens sidegrooved by 25% of the gross thickness, which removes the low crack tip constraint near surface regions and produces a uniform crack-tip constraint across the crack front. The J_f-R curve for other crack-tip constraints (CTC) can be estimated from equation (2).

$$J_f(CTC_2) = J_f(CTC_1) \times \frac{J_i(CTC_2)}{J_i(CTC_1)} \qquad (2)$$

Figure 2 shows the J_S-R curve derived from measured J-R curves and shear-lips for non-sidegrooved specimens, using equations (1) and (2), and

the J_f-R curve obtained from sidegrooved specimens. The J_S-R curve is apparently independent of specimen size and geometry over the crack extension range measured.

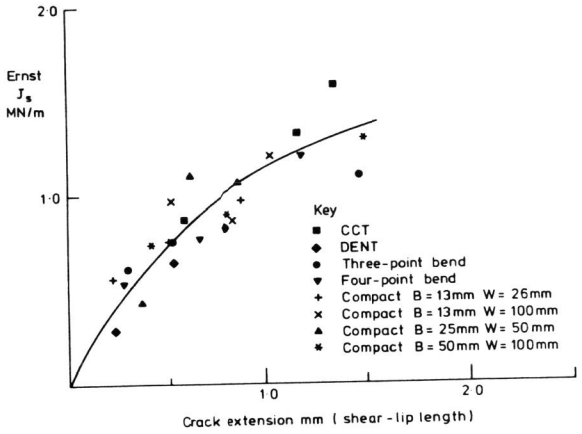

Fig.2 J-R curve for shear-lip region.

For structural applications where a conservative prediction of crack initiation and failure is required, the J_f-R curve can be used, determined either from specimens of an equivalent crack-tip constraint, or indirectly from equation (2). Figure 3 shows J_f-R values for several specimen geometries of the same thickness, calculated from the measured J-R curves and shear-lip sizes using equation (1), and the best fit line to the J_S-R curve shown in Fig. 2. To within experimental scatter, there is no geometry dependence, at least up to 2.5mm of crack extension, which corresponds to 60% of the final ligament size of the tension specimens. An absence of a geometry dependence is consistent with the constant value of the crack opening displacement at the growing crack tip measured in the central region of the specimen (Gibson et al, 1987).

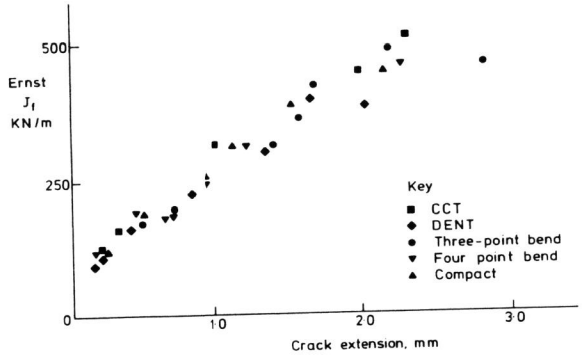

Fig.3 J-R curve for flat fracture region.

When a more accurate assessment of the failure conditions of cracked components is required, it is necessary to include the shear-lip contribution. Figures 4 and 5 show J-R curves predicted using equations (1) and (2) together with measured shear lip sizes, the J_f-R curve determined from sidegrooved specimens and the J_s-R curve given in Fig. 2. The agreement with the experimental data confirms that the observed specimen size and geometry dependence may be calculated using equation (1). However, to predict a J-R curve relevant to a cracked structure, it is necessary to know in advance the relationship between shear-lip size and average crack extension. Such a relationship has been obtained for bend type geometries, when b>B. However, further work is required to develop these relationships for other specimen geometries and crack shapes.

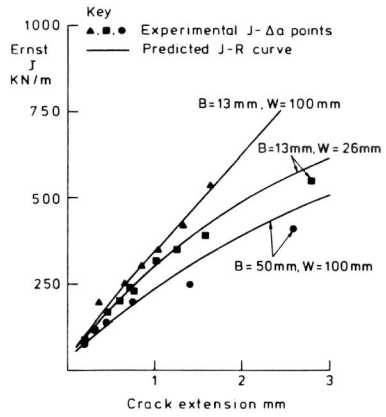

Fig.4 Predicted J-R curves for compact specimens.

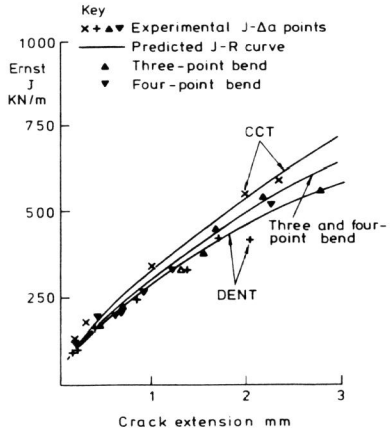

Fig.5 Predicted J-R curves for various specimen geometries.

COMPARISON OF J-R CURVES UNDER CONTAINED AND NON-CONTAINED YIELDING

The results in this section were obtained on an aluminium alloy (BS1474). This material has a relatively low toughness to yield stress ratio, which allows contained yielding conditions to be obtained in relatively small specimens. Tests were carried out on compact specimens (B=10mm, W=20mm and B=25mm, W=50mm) sidegrooved to a depth of either 10 or 25% of the gross thickness.

Crack extension was determined by the AC potential drop (Gibson, 1987 and 1988) technique which involves passing a constant alternating current through the specimen and monitoring changes in the potential drop (PD) across the crack mouth. Figure 6 shows a typical plot of load and PD versus load-line displacement. In addition to crack growth, the PD signal is affected by elastic loading of the specimen. In aluminium alloys, the elastic contribution is linearly proportional to the elastic displacement. As a first step to calculating the amount of crack growth, the PD signals are approximately corrected for elastic loading using the initial specimen compliance. These corrected PD signals are plotted versus the crack tip

opening displacement (CTOD), calculated in accordance with the CTOD testing standard BS5762:1979. Figure 7 shows a typical plot of the initial portion of a corrected PD versus CTOD curve. The onset of crack initiation is indicated by a positive deviation from linearity (Gibson, 1987 and 1988). The amount of crack extension can be determined from the increase in PD using a calibration relationship between PD and crack length which was determined analytically (Gibson, 1987). The same calibration relationship can be used to determine the amount of crack advance due to crack blunting (SZW), except that the increase in PD is divided by π because the increase in current path length through the specimen, and thus PD is related to the circumference of the blunted crack-tip which is πxSZW, assuming a semicircular crack tip profile.

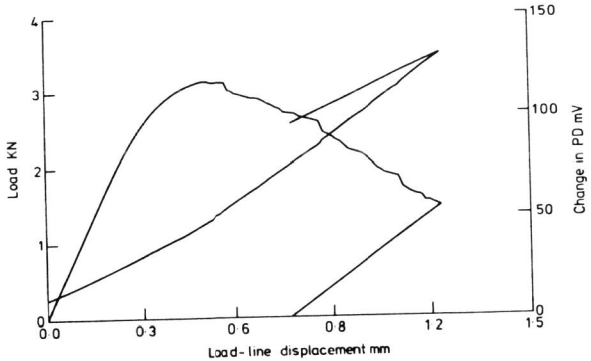

Fig.6 Load and PD versus load-line displacement.

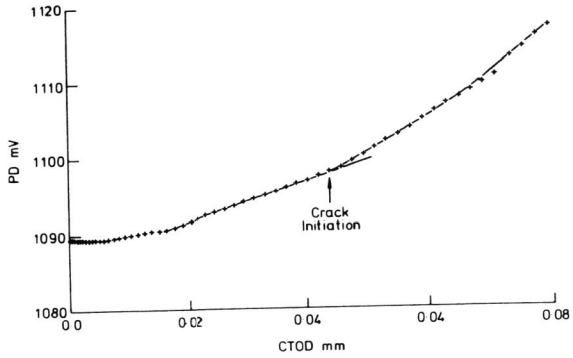

Fig.7 Corrected PD versus CTOD.

Prior to calculating the crack extension, the PD signals are more accurately corrected for the effect of elastic loading using the specimen compliance corresponding to the crack length after the previous increment of crack advance.

Figure 8 shows the J-R curves determined from 10mm thick specimens sidegrooved by 10 and 25% and a 25mm specimen sidegrooved by 10%. In all

cases the final crack extensions were predicted to within 5% of the value measured from the fracture surface. The J-R curve for the 25mm thick specimen was obtained under conditions of contained yielding up to a crack extension of about 1mm. Contained yielding is defined when the load is below that for net section yield (calculated assuming plane strain conditions), which corresponds to a plastic load-line displacement of less than 0.002xW. Crack initiation and subsequent crack growth for the 10mm thick specimens were determined under conditions of non-contained yielding. It can be seen from Figure 8 that to within typical experimental scatter, the J-R curves are the same for both specimen sizes, and thus the same for both contained and non-contained yielding. As the J-R curves for the 10mm thick specimens are approximately the same for both sidegroove depths, and all the measured yield loads corresponded to those for plane strain, it suggests that the level of crack tip constraint was the same in all the specimens.

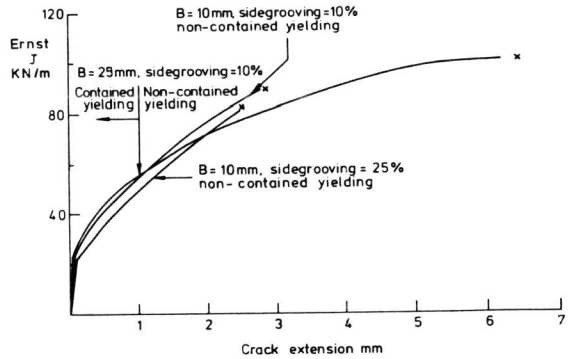

Fig.8 J-R curves for various sized specimens.

These results tentatively suggest that the approach outlined in the previous section can be used to predict J-R curves for large cracked structures under contained yielding from the results from test specimens under non-contained yielding.

SUMMARY

It has been shown that the J-R curve for non-sidegrooved specimens can be predicted from the J-R curves for the shear-lip and flat fracture regions, knowing the relationship between shear-lip size and average crack extension. It has also been demonstrated that the initial region of the J-R curve is the same under both contained and non-contained yielding. It should be possible to predict the J-R curve for large structures where yielding is contained using results of small specimens under non-contained yielding.

ACKNOWLEDGEMENT

The work described was undertaken as part of the Underlying Research Programme of the UKAEA.

REFERENCES

Davis, D.A., M.G. Vassilaros and J.P. Gudas. (1983). Specimen geometry and extended crack growth effects on J_i-R curve characteristics for HY-130 and ASTM A533B Steels. ASTM STP 803, ASTM, II 582-610.

Druce, S.C. (1981). Effect of specimen geometry on the characterisation of ductile crack extension in C-Mn steel. ICF5, 2, Pergamon Press, 843-854.

Ernst, H.A. (1983). Material resistance and instability beyond J-controlled crack growth. ASTM STP 803, ASTM, I 191-213.

Garwood, S.J. (1982). Geometry and orientation effects on ductile crack growth resistance. Int. J. Pres. and Piping, 10, 297-319.

Gibson, G.P. (1987). The use of alternating current potential drop for determining J-crack resistance curves. Eng. Fracture Mech., 26, 213-222.

Gibson, G.P. (1988). Evaluation of the AC potential drop method to determine J-crack resistance curves for a pressure vessel steel. To be published in Eng. Fracture Mech.

Gibson, G.P., S.G. Druce. (1987). An assessment of various crack tip displacement based elastic-plastic fracture parameters to characterise ductile crack growth resistance. Inst. J. of Fracture, 35, 139-151.

Gibson, G.P., S.G. Druce and C.E. Turner. (1987). Effect of specimen size and geometry on ductile crack growth resistance in a C-Mn steel. Inst. J. of Fracture, 32, 219-240.

Hancock, J.W. and D.K. Brown. (1980). The role of the state of stress on crack tip failure processes. Met. Sci., 8 & 9, 293-304.